HHS Public Access

Author manuscript

Calcif Tissue Int. Author manuscript; available in PMC 2018 April 01.

Published in final edited form as:

Calcif Tissue Int. 2017 April ; 100(4): 361–373. doi:10.1007/s00223-016-0225-4.

Bone Mass and Strength are Significantly Improved in Mice Overexpressing Human WNT16 in Osteocytes

Imranul Alam[a,*], **Austin M. Reilly**[a], **Mohammed Alkhouli**[a], **Rita L. Gerard-O'Riley**[a], **Charishma Kasipathi**[a], **Dana K. Oakes**[a], **Weston B. Wright**[a], **Dena Acton**[a], **Amie K. McQueen**[a], **Bhavmik Patel**[a], **Kyung-Eun Lim**[c], **Alexander G. Robling**[c], and **Michael J. Econs**[a,b]

[a]Medicine, Indiana University School of Medicine, IN, USA

[b]Medical and Molecular Genetics, Indiana University School of Medicine, IN, USA

[c]Anatomy and Cell Biology, Indiana University School of Medicine, IN, USA

Abstract

Recently, we demonstrated that osteoblast-specific overexpression of human WNT16 increased both cortical and trabecular bone mass and structure in mice. To further identify the cell-specific role of Wnt16 in bone homeostasis, we created transgenic (TG) mice over-expressing human WNT16 in osteocytes using Dmp1 promoter (Dmp1-hWNT16 TG) on C57BL/6 (B6) background. We analyzed bone phenotypes and serum bone biomarkers, performed gene expression analysis and measured dynamic bone histomorphometry in Dmp1-hWNT16 TG and wild-type (WT) mice. Compared to WT mice, Dmp1-hWNT16 TG mice exhibited significantly higher whole body, spine and femoral aBMD, BMC and trabecular (BV/TV, Tb.N, and Tb.Th) and cortical (bone area and thickness) parameters in both male and female at 12 weeks of age. Femur stiffness and ultimate force were also significantly improved in the Dmp1-hWNT16 TG female mice, compared to sex-matched WT littermates. In addition, female Dmp1-hWNT16 TG mice displayed significantly higher MS/BS, MAR and BFR/BS compared to the WT mice. Gene expression analysis demonstrated significantly higher mRNA level of *Alp* in both male and female Dmp1-hWNT16 TG mice and significantly higher levels of *Osteocalcin, Opg* and *Rankl* in the male Dmp1-hWNT16 TG mice in bone tissue compared to sex-matched WT mice. These results indicate that WNT16 plays a critical role for acquisition of both cortical and trabecular bone mass and strength. Strategies designed to use WNT16 as a target for therapeutic interventions will be valuable to treat osteoporosis and other low bone mass conditions.

[*]**Corresponding author**: Imranul Alam, PhD, Department of Medicine, Indiana University School of Medicine, 1120 West Michigan St, CL459, Indianapolis, IN 46202, Phone (317) 274-0744, Fax (317) 278-0658, ialam@iu.edu.

Disclosure statement: The authors declare that they have no conflict of interest.

Authors' roles

Study design: IA and MJE. Study conduct: IA, AMR, MA, RLG, CK, DKO, WBW, DA, AKM, BP, KL, AGR and MJE. Data analysis: IA, AMR, MA, RLG, CK, DKO, WBW, DA, AKM, BP, AMR, KL and AGR. Data interpretation: IA, AMR, MA, RLG, AGR and MJE. Drafting manuscript: IA, AGR and MJE. Revising manuscript content: IA, AGR and MJE. Approval of final version of manuscript: IA, AMR, MA, RLG, CK, DKO, WBW, DA, AKM, BP, KL, AGR and MJE.

Keywords

WNT16; osteocyte; transgenic; bone mass; gene; osteoporosis

Introduction

Currently, two major therapeutic approaches are available for the treatment of osteoporosis – anabolic and anti-resorptive therapies. While most pharmacological interventions for osteoporosis are targeted to prevent bone resorption, there is only one anabolic therapy (teriparatide or recombinant human parathyroid hormone, analog 1–34 or PTH) currently approved by the FDA aimed at enhancing bone formation (1, 2). However, PTH can be used for a period of only 2 years and needs to be followed by an anti-resorptive drug to preserve bone gain. Also, PTH is contra-indicated in children and patients with a history of skeletal malignancy or Paget's disease (1, 2). Thus, discovery of novel molecules that will enhance bone formation and sustain positive bone balance at clinically relevant fracture sites are needed for the prevention and treatment of osteoporosis and other low bone mass conditions.

Previously, several genome-wide association studies (GWAS) identified common variants in genes in the WNT (Wingless-type mouse mammary tumor virus integration site) signaling pathway associated with bone mineral density (BMD) and risk of fracture (3–6). In addition, multiple GWAS studies demonstrated that genetic variations in WNT16 are associated with BMD and risk of fracture in children and adults across multiple populations (7–10). WNT16 was also found to be associated with bone phenotypes at skeletal sites predominantly affected by osteoporotic fractures (8, 9). Recently, we identified SNPs in WNT16 were associated with peak BMD in premenopausal women (11). The overwhelming evidence from these human GWAS studies for potential regulation of bone homeostasis by WNT16 was further strengthened by the development of animal models with either deletion of Wnt16 globally or conditionally in bone cells (7, 8, 12, 13). Specifically, global Wnt16 knockout mice exhibited significantly lower cortical bone density and strength as well as increased susceptibility to fracture (8, 13), and these mice failed to increase periosteal bone formation in response to mechanical loading (12). Similarly, osteoblast-specific conditional Wnt16 knockout mice displayed decreased bone density, strength and increased porosity, particularly in the cortical bone (13). Together, these results suggest that WNT16 is critical for maintaining bone mass and strength, and that this molecule might be an attractive target for pharmacologic intervention in treating osteoporosis or other low bone mass conditions.

To further identify the role of WNT16 in bone biology, recently, we created transgenic mice overexpressing human *WNT16* in osteoblast, and demonstrated that the transgenic mice displayed increased cortical and trabecular bone mass and structure in both growing and adult age, with robust trabecular phenotype particularly in female mice (14). Further, using transgenic mice overexpressing mouse *Wnt16* in osteoblasts, Movérare-Skrtic S. et al, showed that the transgene had a robust effect on trabecular bone phenotype in adult female mice (15). These results suggest that WNT16 play significant role for acquisition and maintenance of trabecular bone mass in addition to its critical role for cortical bone mass regulation.

The source and target cells of Wnt16 in skeletal tissue are currently mostly unknown. Therefore, we determined the expression of *Wnt16* mRNA in bone cells (osteoblasts, osteocytes and osteoclasts) derived from primary culture. We detected significantly higher expression of *Wnt16* in both osteoblasts (~300 fold) and osteocytes (~30 fold) compared to osteoclasts. Further, Movérare-Skrtic S. et al., showed that substantially lowered *Wnt16* mRNA expression in late osteoblasts and osteocytes led to significantly lower cortical bone thickness in elderly mice (13), suggesting that Wnt16 derived from osteocytes might play an important role in maintenance of bone mass during aging. To further identify the osteocyte-specific role of WNT16 in bone homeostasis, we created transgenic (TG) mice that over-express human *WNT16* in late osteoblasts and osteocytes using Dmp1 (Dentin matrix protein 1) promoter (Dmp1-hWNT16) on C57BL/6 (B6) background. We measured bone density, structure and strength, evaluated serum biomarkers of bone metabolism, performed gene expression analyses and dynamic bone histomorphometry, and analyzed cellular parameters using both male and female Dmp1-hWNT16 TG and wild-type (WT) mice. We demonstrate that WNT16 overexpression in osteocytes influences trabecular and cortical bone mass, structure and strength in mice.

Materials and Methods

Generation of the Dmp1-hWNT16 transgenic mice

The cDNA of human WNT16 (IMAGE clone ID 8143948) cloned into the pCR4-TOPO vector, was obtained from Open Biosystem (PA, USA). The WNT16 gene was excised from this vector by EcoR1 digestion and was cloned into the pBluescript II KS plasmid (pBS-KS) from Agilent Technologies (CA, USA), inserted into the multiple cloning sites between the late osteoblast and osteocyte-specific Dmp1 promoter (8 kb of the 5'-flanking region, the first exon, the first intron and 17 bp of exon2 of the murine *Dmp1* gene, a kind gift from Teresita Bellido) and rabbit beta-globin polyA signal (Figure 1A). The transgene expression construct (Dmp1 promoter + *WNT16* cDNA + polyA tail sequence) was digested with NotI and SalI and microinjected into pronuclei of B6 fertilized eggs, which were then transferred into C57BL/6 (B6) foster mothers by the Indiana University Institutional Transgenic Animal Facility. The integration of the transgene(s) into the genome of founder mice was determined by PCR using tail DNA.

Experimental Animals

We used 10 male and 10 female mice per genotype (Dmp1-hWNT16 TG and wild-type littermates as controls) in this study unless stated specifically otherwise. All mice were generated and maintained at Indiana University. Mice were housed in polycarbonate cages in a vivarium maintained on a 12-h light and 12-h dark cycle and were fed a regular diet and water *ad libitum*. The procedures performed throughout the experiment were in accordance with the ethical standards and guidelines of the Indiana University Animal Care and Use committee (IACUC).

Euthanasia and specimen collection

Mice were euthanized at 12 weeks of age, and lower limbs and lumbar 5 vertebrae were dissected from these animals. The femora on the right side were immediately stored at

−80°C in saline-soaked gauze for subsequent biomechanical testing. The femora on the left side were stripped of muscle, fixed in 10% neutral buffer formalin for 48 hours before transferred to 70% ethyl alcohol and stored at 4°C for densitometry and histomorphometry analyses. In addition, after removing of muscle and periosteum, both ends of the tibia and humeri were cut to flush out the marrow cavity with PBS before transferring them to RNA later stabilization reagent (Qiagen, CA). We also harvested muscle, spleen, heart and kidney tissues from both WT and Dmp1-hWNT16 transgenic mice, which were flash frozen immediately and stored at −80°C until use for gene expression analysis.

Gene expression analysis

Measurements of gene expression were performed by real-time PCR using bone and other organs from both male and female WT and Dmp1-hWNT16 TG mice as described previously (14). All qPCR reactions were performed using the custom-made primer and probe sets from Integrated DNA Technology (IDT, USA) for human *WNT16* (*hWNT16*), endogenous mouse *Wnt16 (Wnt16)*, runt related transcription factor 2 (*Runx2*), alkaline phosphatase (*Alp*), osteocalcin (*OC*), osteoprotegerin (*Opg*) and tumor necrosis factor (ligand) superfamily, member 11 (*Rankl* or *Tnfs11*). We also investigated 1) Wnt signaling pathway canonical genes - beta-catenin (*Ctnnb1*) and Axin 2 (*Axin2*), and 2) Wnt signaling pathway non-canonical genes - jun proto-oncogene (*c-Jun* or *Ap1*), mitogen-activated protein kinase 8 (*Jnk* or *Mapk8*), protein kinase, cAMP dependent, catalytic, alpha (*Pka*), protein kinase C (*Pkc*). Real-time detection of PCR products was accomplished using an ABI PRISM 7900 sequence detector (Applied Biosystem, CA) and normalized to the house-keeping gene beta-Actin.

Dual energy X-ray absorptiometry (DXA)

The whole body, femur and lumbar vertebrae 1 through 5 of the WT and Dmp1-hWNT16 TG mice were scanned using DXA (PIXImus II mouse densitometer; Lunar Corp., Madison, WI, USA) with ultra-high resolution (0.18 × 0.18 mm/pixel) as described previously (14). After completion of the scan of each bone, mutually exclusive region of interest (ROI) boxes were drawn around the bone from which femur aBMD (g/cm^2) and BMC (g) measurements were obtained.

Micro Computer Tomography (μCT) analysis

The femurs and lumbar 5 vertebrae of WT and Dmp1-hWNT16 TG mice were scanned with a high resolution μCT scanner (vivaCT 40, Scanco Medical AG, Switzerland) with an isotropic voxel size of 10.5 μm^3 as described previously (14). In brief, from the scout-view, the growth plate location was identified and trabecular bone measurements consisting of 200 slices (2.1 mm) was completed from about 1 mm below the growth plate. Lumbar 5 vertebrae measurements included the vertebral body from the cephalad to the caudal endplate excluding the cortical bone. For cortical bone analysis, the mid-femur of each bone was determined from the scout-view and a total of 60 slices (30 slices above and 30 slices below the mid-femur) were scanned with the same setting as described previously (14). Finally, 3D and 2D morphometric evaluations were performed for the cortical and trabecular bone from each scan, and bone volume (BV/TV) and structural parameters (trabecular

number, Tb.N; trabecular thickness Tb.Th; trabecular separation, Tb.Sp; cortical bone area, B.Ar/T.Ar; cortical thickness, Ct.Th) were determined.

Biomechanical measurements

Three-point bending measurement of whole-bone strength of femur was performed using an electromechanical test machine (TestResources, MN, USA) as described previously (14). In brief, the femurs were held in place by small preload (<1N) and each bone was loaded to failure in monotonic compression using a crosshead speed of 0.2 mm/s, during which force and displacement measurements were collected every 0.02 s. From the force versus displacement curves, yield force (N), stiffness (N/mm), ultimate force (N) and energy to failure (mJ) were calculated using MTestWR™ software following standard equations (19).

Cortical and Trabecular bone dynamic histomorphometry

Mice were given calcein (15 mg/kg) and alizarin (30 mg/kg) intraperitoneally 10 days and 3 days before euthanasia at 12 weeks of age. Dynamic bone formation parameters were calculated from the femur midshaft for cortical and distal femur secondary spongiosa for trabecular bone by measuring the unlabeled perimeter (nL.Pm), single-labeled perimeter (sL.Pm), double-labeled perimeter (dL.Pm) and the area between the double labeling (dL.Ar) using the Bioquant Osteo system (Bioquant Corp.) as described previously (14). Derived histomorphometric parameters, including mineralizing surface (MS/BS, %), mineral apposition rate (MAR, um/yr) and bone formation rate (BFR/BS, $um^3/um^2/yr$), were calculated using standard procedures recommended by the ASBMR histomorphometry Committee (21).

Cellular parameters

We compared osteoblast perimeter (Ob.Pm; mm), number of osteoblast (N.Ob), osteoblast number over osteoblast perimeter (N.Ob/Ob.Pm), osteoblast surface over bone surface (Ob.S/BS; %) and osteoblast number over bone perimeter (N.Oc/B.Pm) between WT and transgenic female mice. For osteoclast, we measured osteoclast perimeter (Oc.Pm; mm), osteoclast number over osteoclast perimeter (N.Oc/Oc.Pm), osteoclast surface over bone surface (Oc.S/BS; %) and osteoclast number over bone perimeter (N.Oc/B.Pm) in these mice using standard procedures recommended by the ASBMR histomorphometry Committee (21).

Serum biomarkers

Serum levels of mouse osteoprotegerin (OPG) and tumor necrosis factor (ligand) superfamily, member 11 (RANKL) were measured by Enzyme-Linked ImmunoSorbent Assay (ELISA) kits (R&D Systems, MN, USA) according to the manufacturers' instructions. Serum levels of carboxy-terminal collagen crosslinks (CTX), tartrate-resistant acid phosphatase 5, isoform b (TRAcP5b) and pro-collagen 1 intact N-terminal (P1NP) were measured by ELISA kits (Immunodiagnostics Systems, AZ, USA and Biomedical Technologies Inc., MA, USA) per manufacturers' instructions. Serum calcium (Ca), phosphorus (P), blood urea nitrogen (BUN), creatinine (CREA) and alkaline phosphatase (ALP) were measured using the Randox Rx kit (Daytona Analyzer, WV, USA).

Statistical analysis

Quantitative data were expressed as mean ± SEM. Statistical differences between WT and Dmp1-hWNT16 transgenic groups were tested using the unpaired Student's *t* test. Gender and genotype interaction was analyzed by two-way analysis of variance (ANOVA). All statistical analysis was performed using the statistical software package StatView (Abacus Concepts, Inc., Berkeley, CA). The level of significance was set at $p \leq 0.05$.

Results

Dmp1-hWNT16 TG mice had similar body weight and femoral bone length as WT mice

Transgenic WNT16 mice were born with expected frequency and appeared healthy with no discernible growth or morphological defects. Compared to WT mice, transgenic WNT16 mice showed similar body weight (g) in male and female at 6 and 12 weeks of age (Table 1). In addition, the femur length (mm) at 6 and 12 weeks of age did not differ between male WT and transgenic mice (Table 1).

Dmp1-hWNT16 TG mice expressed high levels of hWNT16 in bone tissue

We detected significantly higher ($p<0.0001$) levels of transgene (*hWNT16*) expression in bone tissue compared to other tissues (muscle, spleen, heart and kidney) in the transgenic mice in both male and female (Figure 1B). In addition, the expression of *hWNT16*, as expected, was detectable only in the transgenic mice (Figure 1B). The level of endogenous mouse *Wnt16* mRNA expression in the bone tissue was significantly higher ($p<0.0001$) compared to other tissues (Figure 1C). In addition, *Wnt16* mRNA expression was significantly lower ($p<0.05$) in the transgenic male mice compared to sex-matched WT littermates (Figure 1C).

Dmp1-hWNT16 TG mice exhibited higher whole body, femur and spine aBMD and BMC measured by DXA

Male transgenic WNT16 mice had significantly higher whole body aBMD and BMC (10% and 12%, respectively; $p<0.05$) compared to WT littermates at 6 weeks of age (Figure 2A and Table 1). Similarly, female transgenic mice showed 16% higher whole body aBMD and 21% higher BMC ($p<0.005$) compared to female WT mice at this age. At 12 weeks of age, both male and female transgenic WNT16 mice had significantly higher whole body aBMD (9%, $p<0.001$ and 14%, $p<0.0001$; respectively) and BMC (11%, $p<0.01$ and 21%, $p<0.0001$; respectively) than WT littermates (Figure 2A and Table 1).

Femoral aBMD measured at 12 weeks of age showed significantly higher values for both transgenic male and female mice (12%, $p<0.001$ and 17%, $p<0.0001$; respectively) as compared to WT mice (Table 1). Similarly, femur BMC was 11% higher in male ($p<0.05$) and 15% higher in female ($p<0.01$) Dmp1-hWNT16 TG mice (Table 1). Spine DXA was measured for lumbar 1 through 5 vertebrae at 12 weeks of age. The spine aBMD in transgenic mice was 14% higher ($p<0.001$) in male and 20% higher ($p<0.0001$) in female compared to WT mice (Figure 2B and Table 1). Similarly, spine BMC was 15% higher in male ($p<0.05$) and 26% higher in female ($p<0.0001$) Dmp1-hWNT16 TG mice (Table 1).

Dmp1-hWNT16 TG mice displayed higher bone mass and improved micro-architecture in cancellous and cortical bone measured by μCT

To further identify the effects of the hWNT16 transgene on skeletal properties in greater detail, we measured bone mass and micro-architectural properties in the distal femur and lumbar 5 vertebra for cancellous bone and at the femoral midshaft for the cortical bone in 12-week-old mice using μCT. Male Dmp1-hWNT16 transgenic mice displayed 2-fold higher ($p<0.0005$) trabecular BV/TV whereas female transgenic mice exhibited 5-fold increase ($p<0.0001$) in BV/TV at distal femur compared to their WT littermates (Figures 3A & 3B). Male Dmp1-hWNT16 TG mice also showed 29% higher Tb.N ($p<0.001$) and 21% higher Tb.Th ($p<0.001$) and 23% lower Tb.Sp ($p<0.005$) whereas female Dmp1-hWNT16 TG mice exhibited 50% higher Tb.N ($p<0.0001$) and 50% higher Tb.Th ($p<0.0001$) and 35% lower Tb.Sp ($p<0.0001$) at the same site (Figures 3A & 3B). Cortical bone morphometry at mid-femur revealed that male Dmp1-hWNT16 TG mice had 11% higher B.Ar/T.Ar ($p<0.05$) and 4% higher Ct.Th ($p<0.005$) whereas female transgenic mice exhibited 10% higher B.Ar/T.Ar ($p<0.0001$) and 6% higher Ct.Th ($p<0.0005$) compared to sex-matched WT mice (Figures 4A & 4B). At lumbar 5 vertebra, male Dmp1-hWNT16 transgenic mice displayed 44% higher ($p<0.001$) trabecular BV/TV whereas female transgenic mice exhibited 122% higher ($p<0.0001$) in BV/TV compared to their WT littermates (Figures 5A). Male Dmp1-hWNT16 TG mice also showed 18% higher Tb.N ($p<0.005$) and 19% higher Tb.Th ($p<0.005$) and 15% lower Tb.Sp ($p<0.005$) whereas female Dmp1-hWNT16 TG mice exhibited 42% higher Tb.N ($p<0.0001$) and 39% higher Tb.Th ($p<0.0001$) and 29% lower Tb.Sp ($p<0.0001$) at the same site (Figures 5B–5D). Two-way ANOVA (gender and genotype interaction) analysis showed sex-specific differences for trabecular ($p<0.005$) bone phenotypes both at distal femur and lumbar 5 vertebra in the Dmp1-hWNT16 TG mice. Overall, these data indicate that while no differences were observed between male and female Dmp1-hWNT16 TG mice in the cortical compartment, female transgenic mice displayed a more pronounced effect of the transgene than did male mice in the cancellous compartment.

Serum markers of bone formation and resorption are not significantly influenced in Dmp1-hWNT16 TG mice

To understand potential changes in serum biochemistry induced by transgenic overexpression of WNT16 in bone, we measured biomarkers related to skeletal metabolism in serum samples collected from 12-week-old mice. Dmp1-hWNT16 TG mice showed similar levels of calcium, phosphorus, BUN and creatinine compared to their WT littermates in both male and female (Table 2). Two serum markers of bone formation, ALP and P1NP, did not differ significantly between the WT and Dmp1-hWNT16 TG in both sexes. In addition, we detected similar levels of serum OPG and RANKL for both genotypes in male and female mice. Further, serum bone resorption markers CTX, TRAcP5b and CTX/TRAcP5b levels did not differ significantly in the transgenic mice compared to WT mice in both sexes (Table 2).

Biomechanical properties of femoral diaphysis are improved in Dmp1-hWNT16 TG mice

To identify whether the higher bone mass and better micro-architecture in Dmp1-hWNT16 mice were associated with improvements in mechanical properties of the skeleton, we tested

femurs from Dmp1-hWNT16 TG and WT mice using monotonic 3-point bending tests. Female Dmp1-hWNT16 TG mice had significantly higher yield force (10%; p=0.01), stiffness (11%; p=0.01), ultimate force (17%; p=0.006) and energy to ultimate force (35%; p=0.02) as compared to female WT mice (Figure 6). In contrast, male Dmp1-hWNT16 TG mice exhibited similar values for stiffness, ultimate force and energy to ultimate force compared to sex-matched WT mice (Figure 6).

Trabecular bone formation rate, mineral apposition rate and mineralizing surface are significantly increased by hWNT16 overexpression in female Dmp1-hWNT16 TG mice

To determine whether greater cortical and trabecular bone volume in Dmp1-hWNT16 TG mice was driven by enhanced bone formation, we measured dynamic bone formation parameters in the femur midshaft and distal femur secondary spongiosa using fluorochrome labels embedded in the bone prior to sacrifice at 12 weeks of age. We compared mineralizing surface (MS/BS), mineral apposition rate (MAR) and bone formation rate (BFR/BS) between sex-matched WT and Dmp1-hWNT16 TG mice. Both male and female transgenic mice had significantly higher MS/BS (22%, $p<0.05$ and 192%, $p<0.0005$; respectively) than their sex-matched WT littermates in the distal femur (Figure 7A). Female transgenic mice also had 28% higher MAR ($p<0.01$) compared to WT female littermates (Figure 7B). In addition, BFR/BS in female transgenic mice were significantly higher (285%; $p<0.0005$) than in sex-matched control WT mice (Figure 7C). In femur midshaft, male and female Dmp1-hWNT16 transgenic mice displayed similar values for periosteal MS/BS, MAR and BFR/BS compared to sex-matched WT littermates (Figure 7D–F). In addition, endosteal MS/BS, MAR and BFR/BS values in transgenic mice did not differ from WT control mice in both sexes (data not shown).

Higher expression of bone formation related genes are observed in the transgenic mice

Significantly higher mRNA levels of *Alp* (64% in male and 3-fold in female; $p<0.05$) and a non-significant higher levels of *Runx2* (22% in male and 59% in female; p=0.1) were observed in the long bone of the transgenic mice compared to their WT littermates (Figure 8A and 8B). The level of *Osteocalcin* expression was significantly higher (84%; $p<0.05$) in male and 37% higher in female transgenic mice (Figure 8C). In addition, 3-fold higher expression of *Opg* and 2-fold higher expression of *Rankl* were detected in the transgenic mice compared to WT mice (Figure 8D and 8E) in male. The levels of *Ctnnb1* expression was 52% higher in the male transgenic mice compared to male WT littermates (Figure 8F). In addition, mRNA expression levels of *c-Jun/Ap1*, *Jnk/Mapk8*, *Pka* and *Pkc* did not differ between the WT and Dmp1-hWNT16 TG mice in both male and female (data not shown).

Osteoblast and osteoclast number and surface area are not significantly changed by hWNT16 overexpression

Transgenic female mice displayed similar values for N.Ob, Ob.Pm, N.Ob/B.Pm and Ob.S/BS compared to sex-matched WT mice (Supplemental Figure 1A–C). In addition, N.Oc, Oc.Pm, N.Oc/B.Pm and Oc.S/BS did not differ between two genotypes (Supplemental Figure 1A, 1B and 1D).

Discussion

The goal of this study was to identify the role of osteocyte-specific overexpression of human WNT16 on bone phenotypes in growing and adult mice. We detected significantly higher whole-body and site-specific (femur and spine) aBMD and BMC, and major improvement of micro-architectural properties of cancellous and cortical bone in the femur in both male and female transgenic mice. In addition, we found a milder cortical bone phenotype and a superb cancellous bone phenotype in transgenic mice in both sexes. Further, striking sex-specific phenotypic differences were observed in the transgenic mice, with more pronounced effect of the transgene in female mice in cancellous bone and substantial improvement of bone biomechanical properties in female, compared to male transgenic mice. Together, these results suggest that WNT16 has a marked positive effect for regulation of both cortical and trabecular bone mass and strength.

Both growing and adult Dmp1-hWNT16 TG mice displayed similar body weight and femur length as compared to WT mice, however, phenotypic differences for aBMD and BMC were clearly noticeable as early as 4 weeks of age between the two genotypes. Additionally, values for DXA and microCT derived bone phenotypes in transgenic mice were superior at both axial (lumbar spine) and appendicular (femur) skeletal sites compared to their WT counterparts. Bone phenotypes were also more pronounced in females and the phenotypic differences between wild-type and transgenic mice were maintained to the adult age. Sex-specific differences between Dmp1-hWNT16 TG mice were also observed in the femur three-point bending test and bone histomorphometric measurements. Female Dmp1-hWNT16 TG displayed superior biomechanical properties of femur and substantial improvement of dynamic bone formation parameters at the trabecular site compared to male transgenic mice.

Compared to our previous osteoblast-specific overexpression of WNT16 study (14) and another study using similar mouse model (15), the current study showed that osteocyte-specific overexpression of WNT16 increased similar extent of aBMD in whole body and spine, however, we observed lower magnitude of trabecular BV/TV increase at distal femur in both male and female Dmp1-hWNT16 transgenic mice. This could be due to transgene expression differences in osteocytes versus osteoblasts at this skeletal site in these mouse models. Also, mouse *Wnt16* mRNA was decreased only in the male Dmp1-hWNT16 transgenic bone compared to WT bone, suggesting that transgenic mice might process endogenous *Wnt16* mRNA differently. In addition, in the male Col2.3-WNT16 transgenic mice, expression of *Opg* in bone tissue was significantly increased whereas no changes were observed in the *Rankl* expression leading to higher *Opg/Rankl* ratio in the transgenic mice (14). In contrast, while mRNA level of *Opg* was increased 3-fold, expression of *Rankl* was also increased 2-fold in the male Dmp1-hWNT16 transgenic mice, resulting in no changes of *Opg/Rankl* ratio in the transgenic mice compared to sex-matched wild-type mice, suggesting a higher level of bone turnover in the transgenic mice. Further, while the N.Oc/B.Pm and Oc.S/BS were significantly lower in the Col2.3-WNT16 transgenic mice (14), these values were similar in the Dmp1-hWNT16 transgenic mice compared to sex-matched wild-type mice. On the other hand, Movérare-Skrtic S. et al. found no significant changes of bone formation or resorption markers in mice overexpressing WNT16 in osteoblasts (15).

These discrepancies might be related to the different levels of transgenes produced by osteoblasts and osteocytes as well as the type of interactions, for example, paracrine or autocrine, among these bone cells with osteoclasts and other cells in the bone tissue. Our finding in the current study is in agreement with a previous study demonstrating that the periosteal BFR and MAR were significantly reduced in female Wnt16 knockout mice compared to wild-type mice at 12 weeks of age (12). However, in another study (13), a non-significant trend of lower periosteal MAR at 6 weeks of age and no changes of periosteal MAR at 12 weeks of age was observed in Wnt16 knockout mice, which could be due to the different bones (tibia versus femur) used for histomorphometric measurements.

Striking differences of bone phenotypes detected between male and female in the WNT16 transgenic mice were in concert with those observed in the Wnt16 knockout mice. Several studies demonstrated that global deletion of Wnt16 in female mice decreased cortical bone volume and thickness, increased cortical porosity, and resulted in spontaneous fractures at multiple skeletal sites (7, 8, 13). Recently, conditional deletion of Wnt16 from osteoblast-lineage cells also revealed that Wnt16 is a critical regulator for maintenance of cortical bone mass and fracture susceptibility in female mice (13). In addition, female Wnt16 knockout mice failed to increase periosteal bone formation in response to mechanical loading (12). This sex-specific bone phenotype differences were also observed in Col2.3-WNT16 (14) and Dmp1-hWNT16 transgenic mice. In concert, Movérare-Skrtic S. et al., recently demonstrated that osteoblast-specific overexpression of mouse *Wnt16* predominantly increased trabecular bone mass in female mice (15). Together, these results strongly suggest the potential role of sex-hormones mediating the effect of Wnt16 transgene for bone homeostasis. Recently, using two genetically modified mouse models (Wnt16 knockout and osteoblast-specific Wnt16 overexpression), Movérare-Skrtic S. et al., demonstrated that although Wnt16 mRNA expression is enhanced by estradiol treatment, the bone-sparing effects of estrogen and WNT16 are independent of each other (15). In addition, Todd H. et al., found that estrogen deficiency or ovariectomy decreased expression of Wnt16 whereas estrogen replacement using 17b-estradiol and the Selective Estrogen Receptor Modulator Tamoxifen increased expression of Wnt16 in the cortical bone in mice (16), suggesting potential interactions between Wnt16 and estrogen for overall bone mass regulation. Further studies are thus necessary to decipher the complex interplay between estrogen and Wnt16 for regulation of bone homeostasis.

The WNT signaling pathway plays a major role in embryonic development and postnatal health and diseases, including bone and mineral homeostasis (17–20). Studies involving both global and conditional deletion of Wnt16 from osteoblast-lineage cells in mice revealed that Wnt16 is a critical regulator for maintenance of cortical bone mass and fracture susceptibility (7, 8, 13). In a previous study, we observed a robust trabecular bone phenotype in the Col2.3-WNT16 transgenic (overexpressing human *WNT16* in osteoblasts) mice in both males and females (14). More recently, Movérare-Skrtic S. et al., demonstrated that osteoblast-specific overexpression of mouse *Wnt16* predominantly increased trabecular bone mass in female mice at 16 weeks of age (15). In the current study, we further observed superb cancellous bone phenotype in male and female Dmp1-hWNT16 transgenic mice. This drastic difference of cortical bone phenotypes in the Wnt16 knockout mouse models (global and conditional) versus predominant trabecular bone phenotypes in the Dmp1-

hWNT16 (current study) and Col2.3-WNT16 (14) overexpression mouse models might result from various factors including 1) interactions of complex signaling among several Wnts and their intracellular and extracellular modulators, 2) differences in bone micro-environment, 3) influences of mechanical signals perceived by the tissue, and 4) cross-talk of Wnt signaling with other signaling pathways. In addition, levels of endogenous *Wnt16* mRNA expression might vary between cortical and trabecular bone as it has been shown previously (15). This could lead to different dose-response curves proposed recently between Wnt16 expression and bone mass in these two compartments (15). These results are in consistent with previous human GWAS studies demonstrating the association between WNT16 and BMD at skeletal sites with predominant trabecular bone such as spine and heel (5, 10, 11). Overall these data suggest that WNT16 exerts distinct effect on compartment-specific bone mass, depending on whether it is perturbed physiologically (knockout of Wnt16) or manipulated pharmacologically (overexpression of WNT16). Up-regulation of Wnt16 as a pharmacological approach may therefore have great potential for treating conditions with substantial trabecular bone loss such as post-menopausal osteoporosis and glucocorticoid induced bone loss.

This study has several limitations. We did not measure bone phenotypes in mice older than 12 weeks of age, therefore, whether the transgenic mice will preserve higher bone mass and strength as they age needs to be explored in future. Also, we have not investigated the effect of mechanical loading or unloading on bone phenotypes in our transgenic mouse model. Moreover, as strong sex-specific differences were observed in the transgenic mice, whether and how sex hormones contribute to the overall bone homeostasis in these mice needs further investigation.

In conclusion, we demonstrated that Dmp1-hWNT16 transgenic mice exhibited significantly higher total body, spine and femoral bone mineral density in both male and female mice. Bone volume and micro-architecture at trabecular sites were also significantly improved in the transgenic mice, particularly in female. Cortical bone areas and thickness were modestly improved in the transgenic mice in both sexes, and bone biomechanics was substantially improved in the female transgenic mice. Our data indicate that WNT16 is critical for the acquisition of both cortical and trabecular bone mass and strength, and that this molecule might be targeted for therapeutic interventions to treat osteoporosis or other low bone mass and high bone-fragility conditions.

Supplementary Material

Refer to Web version on PubMed Central for supplementary material.

Acknowledgments

This work was supported by the US National Institutes of Health grants AG041517 and AR053237, and Veteran's Administration grant BX001478.

References

1. Rachner TD, Khosla S, Hofbauer LC. Osteoporosis: now and the future. Lancet. 2011; 377(9773): 1276–1287. [PubMed: 21450337]

2. Lewiecki EM. New targets for intervention in the treatment of postmenopausal osteoporosis. Nat Rev Rheumatol. 2011; 7(11):631–638. [PubMed: 21931340]
3. Estrada K, Styrkarsdottir U, Evangelou E, et al. Genome-wide meta-analysis identifies 56 bone mineral density loci and reveals 14 loci associated with risk of fracture. Nat Genet. 2012; 44(5): 491–501. [PubMed: 22504420]
4. Berndt SI, Gustafsson S, Mägi R, et al. Genome-wide meta-analysis identifies 11 new loci for anthropometric traits and provides insights into genetic architecture. Nat Genet. 2013; 45(5):501–512. [PubMed: 23563607]
5. Moayyeri A, Hsu YH, Karasik D, et al. Genetic determinants of heel bone properties: genome-wide association meta-analysis and replication in the GEFOS/GENOMOS consortium. Hum Mol Genet. 2014; 23(11):3054–3068. [PubMed: 24430505]
6. Kemp JP, Medina-Gomez C, Estrada K, et al. Phenotypic dissection of bone mineral density reveals skeletal site specificity and facilitates the identification of novel loci in the genetic regulation of bone mass attainment. PLoS Genet. 2014; 10(6):e1004423. [PubMed: 24945404]
7. Medina-Gomez C, Kemp JP, Estrada K, et al. Meta-analysis of genome-wide scans for total body BMD in children and adults reveals allelic heterogeneity and age-specific effects at the WNT16 locus. PLoS Genet. 2012; 8(7):e1002718. [PubMed: 22792070]
8. Zheng HF, Tobias JH, Duncan E, et al. WNT16 influences bone mineral density, cortical bone thickness, bone strength, and osteoporotic fracture risk. PLoS Genet. 2012; 8(7):e1002745. [PubMed: 22792071]
9. García-Ibarbia C, Pérez-Núñez MI, Olmos JM, et al. Missense polymorphisms of the WNT16 gene are associated with bone mass, hip geometry and fractures. Osteoporos Int. 2013; 24(9):2449–2454. [PubMed: 23417354]
10. Hendrickx G, Boudin E, Fijałkowski I, et al. Variation in the Kozak sequence of WNT16 results in an increased translation and is associated with osteoporosis related parameters. Bone. 2014; 59:57–65. [PubMed: 24185276]
11. Koller DL, Zheng HF, Karasik D, et al. Meta-analysis of genome-wide studies identifies WNT16 and ESR1 SNPs associated with bone mineral density in premenopausal women. J Bone Miner Res. 2013; 28(3):547–558. [PubMed: 23074152]
12. Wergedal JE, Kesavan C, Brommage R, Das S, Mohan S. Role of WNT16 in the regulation of periosteal bone formation in mice. Endocrinology. 2015; 156(3):1023–1032. [PubMed: 25521583]
13. Movérare-Skrtic S, Henning P, Liu X, et al. Osteoblast-derived WNT16 represses osteoclastogenesis and prevents cortical bone fragility fractures. Nat Med. 2014; 20(11):1279–1288. [PubMed: 25306233]
14. Alam I, Alkhouli M, Gerard-O'Riley, et al. Osteoblast-specific overexpression of human WNT16 increases both cortical and trabecular bone mass and structure in mice. Endocrinology. 2016; 157(2):722–736. [PubMed: 26584014]
15. Movérare-Skrtic S, Wu J, Henning P, et al. The bone-sparing effects of estrogen and WNT16 are independent of each other. Proc Natl Acad Sci USA. 2015; 112(48):14972–14977. [PubMed: 26627248]
16. Todd H, Galea GL, Meakin LB, et al. Wnt16 is associated with age-related bone loss and estrogen withdrwal in murine bone. PLoS One. 2015; 10(10):e0140260. [PubMed: 26451596]
17. Clevers H, Nusse R. Wnt/β-catenin signaling and disease. Cell. 2012; 149(6):1192–1205. [PubMed: 22682243]
18. Cadigan KM, Peifer M. Wnt signaling from development to disease: insights from model systems. Cold Spring Harb Perspect Biol. 2009; 1(2):a002881. [PubMed: 20066091]
19. Logan CY, Nusse R. The Wnt signaling pathway in development and disease. Annu Rev Cell Dev Biol. 2004; 20:781–810. [PubMed: 15473860]
20. Baron R, Kneissel M. WNT signaling in bone homeostasis and disease: from human mutations to treatments. Nat Med. 2013; 19(2):179–192. [PubMed: 23389618]
21. Dempster DW, Compston JE, Drezner MK, et al. Standardized nomenclature, symbols, and units for bone histomorphometry: a 2012 update of the report of the ASBMR Histomorphometry Nomenclature Committee. J Bone Miner Res. 2013; 28(1):2–17. [PubMed: 23197339]

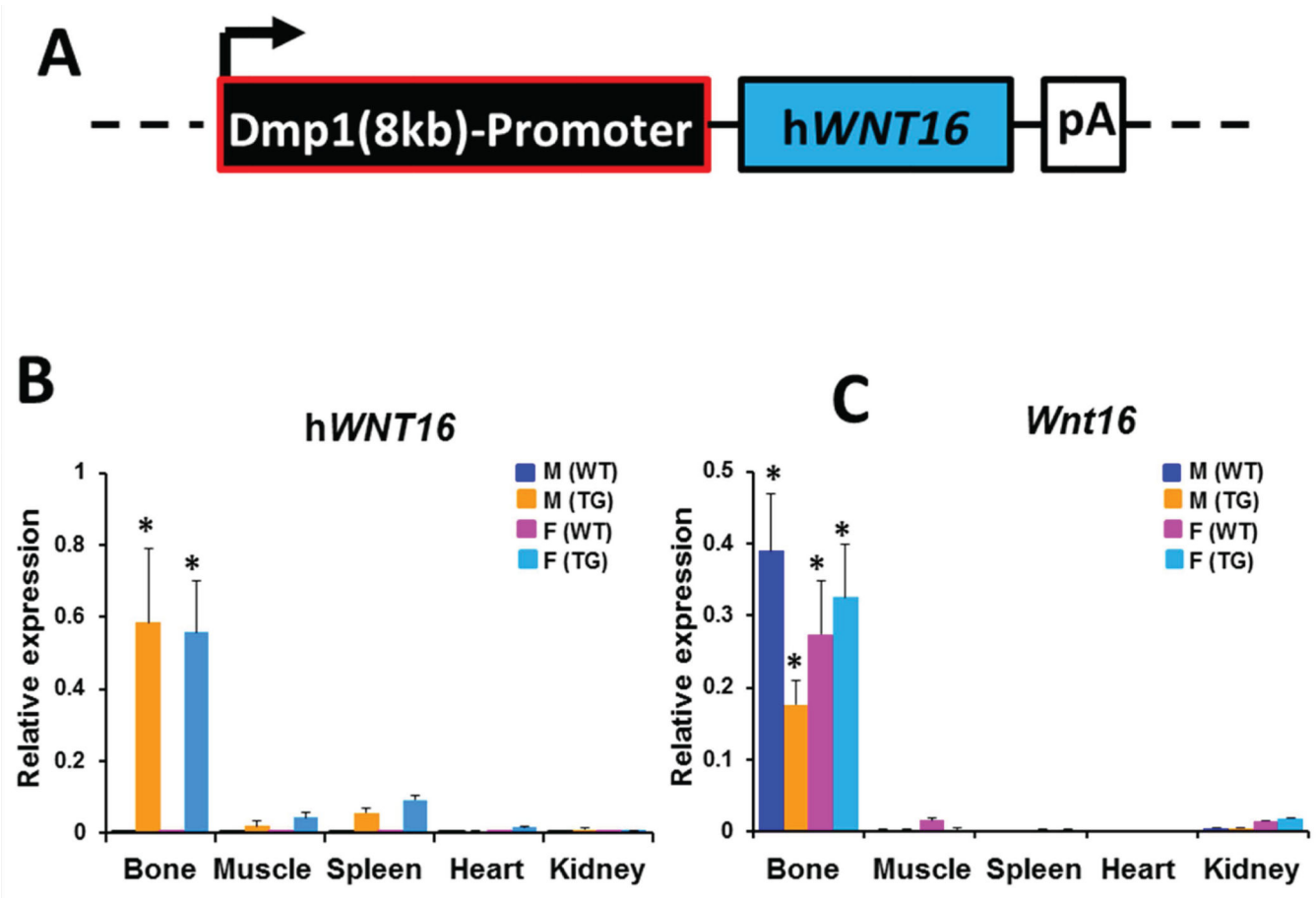

Fig. 1.

Generation and characterization of the Dmp1-hWNT16 transgenic mice. The human WNT16 (hWNT16) cDNA was cloned into the pBluescript II KS plasmid (pBS-KS) between the osteocyte-specific Dmp1 promoter (8 kb of the 5'-flanking region, the first exon, the first intron and 17 bp of exon2 of the murine *Dmp1* gene, a kind gift from Teresita Bellido) and rabbit beta-globin polyA signal (1A). Higher level of transgene (hWNT16) was observed in bone tissue compared to other tissues (muscle, spleen, heart and kidney) in transgenic mice measured by real-time PCR (1B). A high level of transgene (hWNT16) mRNA expression was detected only in the transgenic mice (1B). The level of endogenous mouse *Wnt16* mRNA expression in the bone tissue was significantly higher compared to other tissues (1C). Values are given as mean ± SEM *$p<0.0001$ vs. corresponding WT using Student's t test. WT: wild-type; TG: Dmp1-hWNT16 transgenic

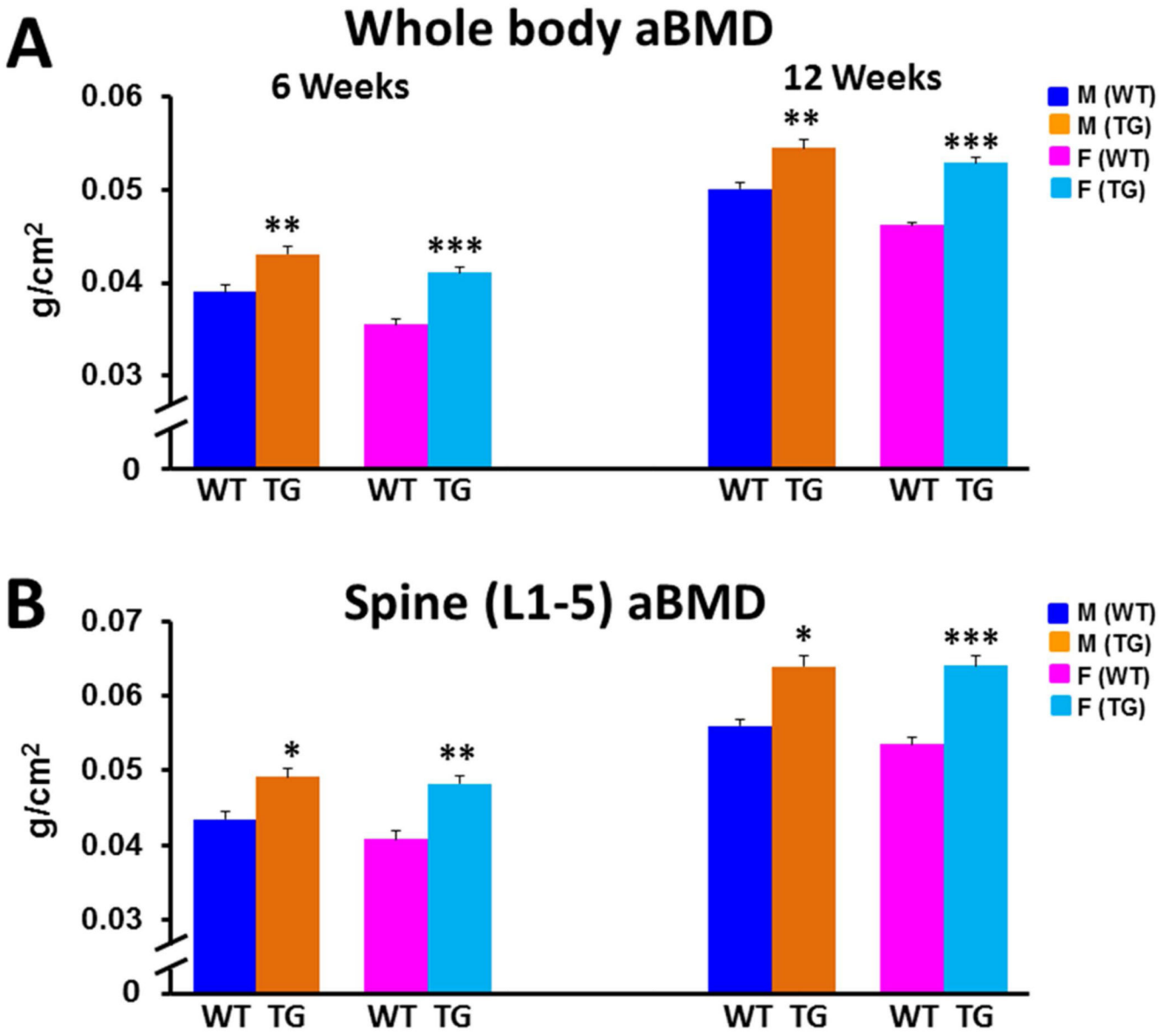

Fig. 2.

Whole body and spine (L1–5) aBMD measured by DXA. Both male and female transgenic Dmp1-hWNT16 transgenic mice exhibited significantly higher whole body (2A) and spine (2B) aBMD at 6 and 12 weeks of age compared to age- and sex-matched WT mice. Values are given as mean ± SEM *p<0.05; **p<0.0005; ***p<0.0001 vs. corresponding WT using Student's t test. WT: wild-type; TG: Dmp1-hWNT16 transgenic

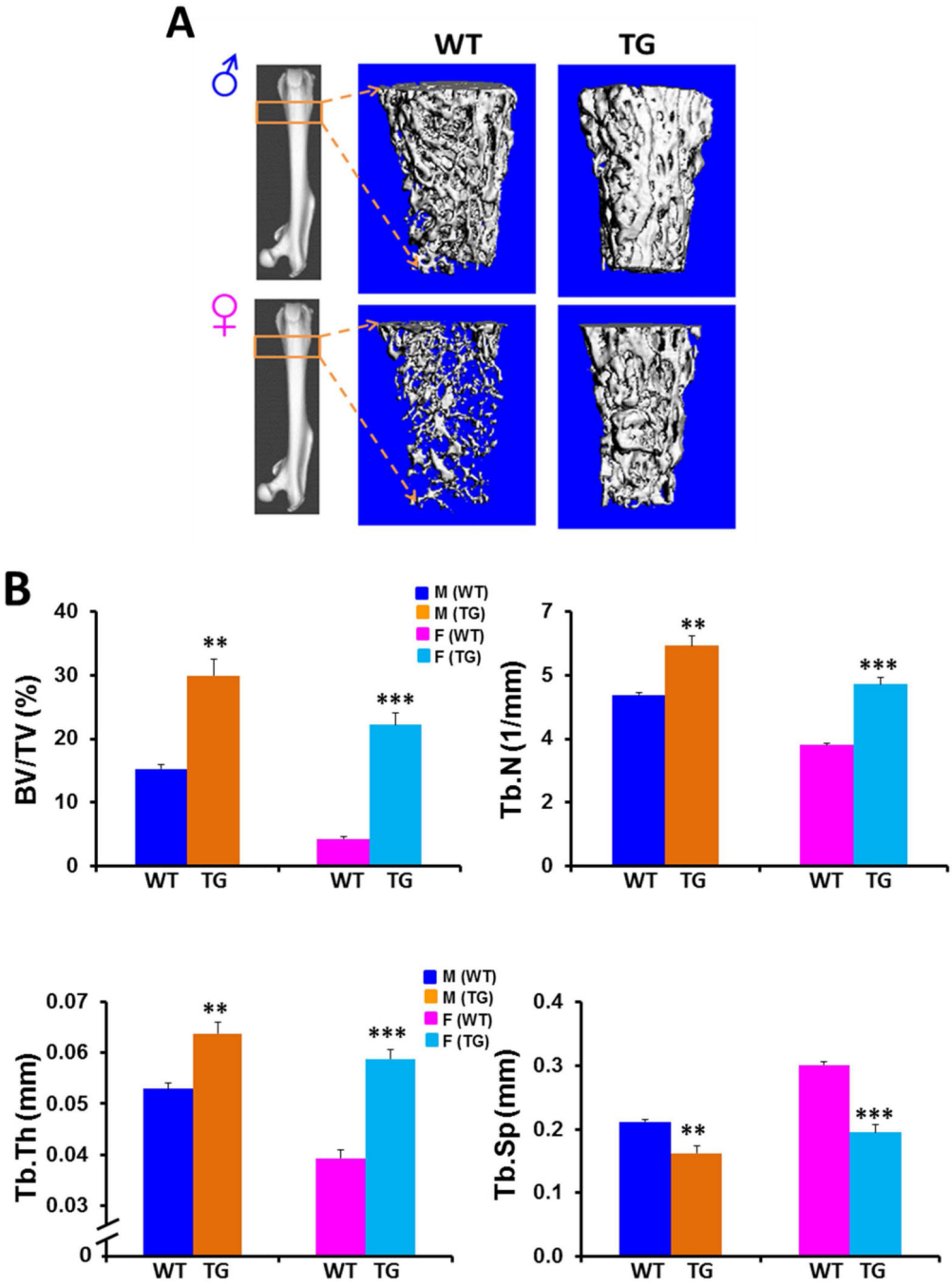

Fig. 3.

Trabecular bone morphometry measured by micro-CT. Representative μCT pictures at distal femur in male and female WT and Dmp1-hWNT16 transgenic mice (3A). Compared to WT mice, Dmp1-hWNT16 transgenic mice at 12 weeks of age showed significantly higher trabecular bone volume (BV/TV), trabecular number (Tb.N) and trabecular thickness (Tb.Th), but significantly lower trabecular separation (Tb.Sp) at distal femur in both male and female (3B). Values are given as mean ± SEM *p<0.05; **p<0.0005; ***p<0.0001 vs. corresponding WT using Student's t test. WT: wild-type; TG: Dmp1-hWNT16 transgenic

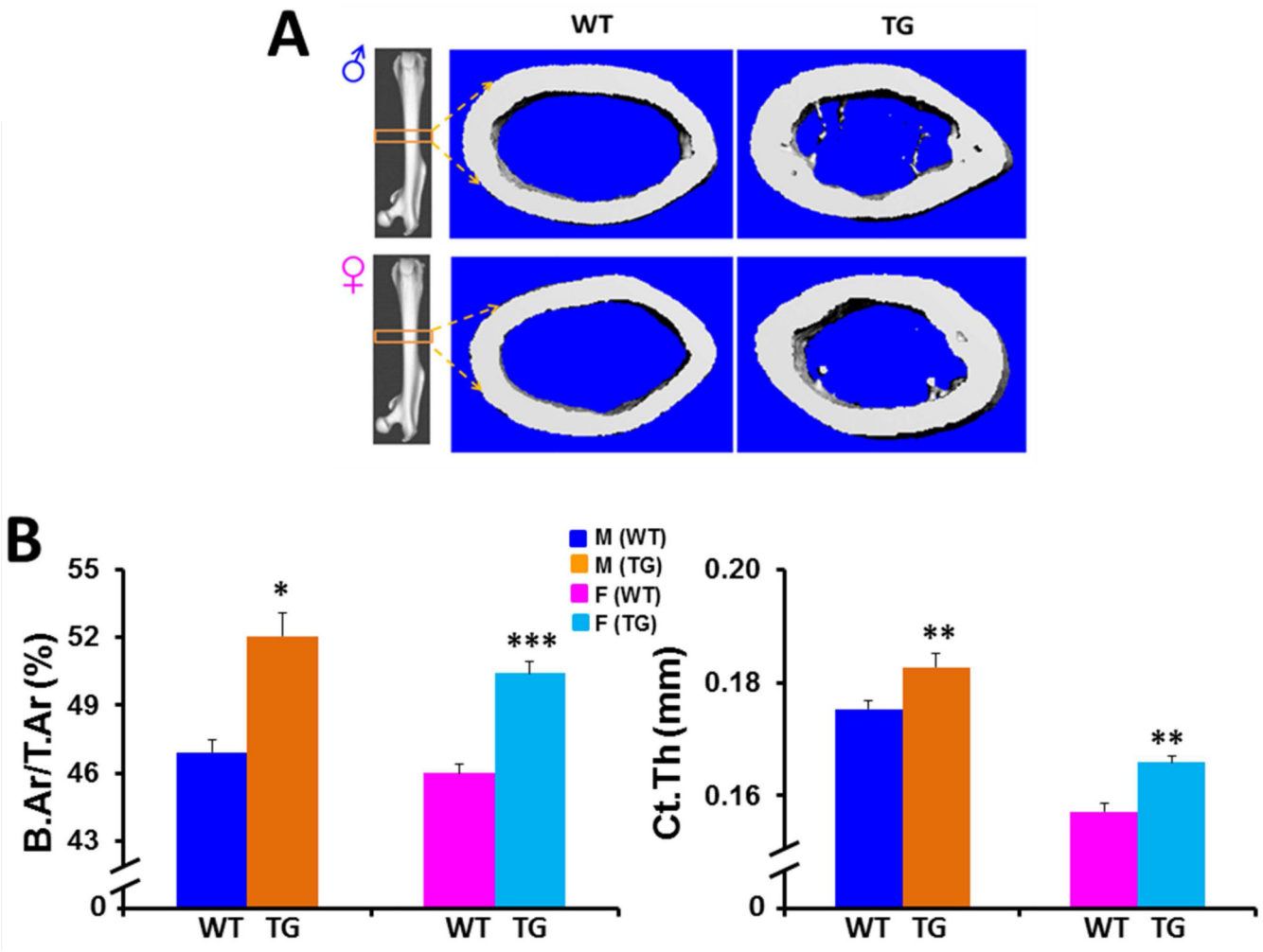

Fig. 4.

Cortical bone morphometry measured by micro-CT. Representative μCT pictures at femur midshaft in male and female WT and Dmp1-hWNT16 transgenic mice (4A). Male and female Dmp1-hWNT16 transgenic mice showed significantly higher cortical bone area (B.Ar/T.A) and cortical thickness (Ct.Th) compared to their sex-matched WT littermates at 12 weeks of age (4B). Values are given as mean ± SEM *$p<0.05$; **$p<0.0005$; ***$p<0.0001$ vs. corresponding WT using Student's t test. WT: wild-type; TG: Dmp1-hWNT16 transgenic

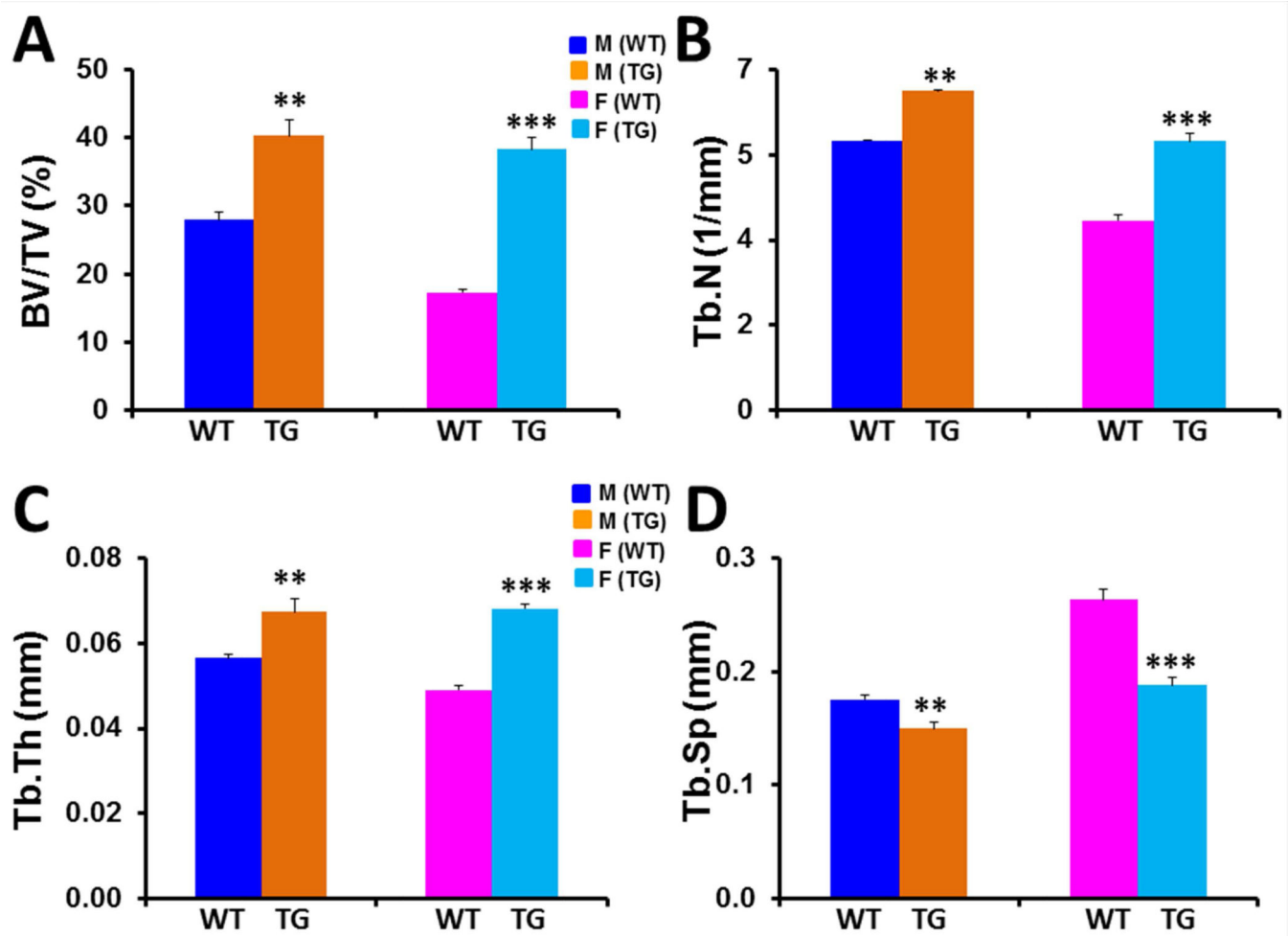

Fig. 5.

Trabecular bone morphometry at lumbar 5 vertebra measured by micro-CT. Compared to WT mice, Dmp1-hWNT16 transgenic mice at 12 weeks of age showed significantly higher trabecular bone volume (BV/TV) (5A), trabecular number (Tb.N) (5B) and trabecular thickness (Tb.Th) (5C), but significantly lower trabecular separation (Tb.Sp) (5D) at lumbar 5 vertebra in both male and female. N=6 per sex per genotype. Values are given as mean ± SEM **p<0.005; ***p<0.0001 vs. corresponding WT using Student's t test. WT: wild-type; TG: Dmp1-hWNT16 transgenic

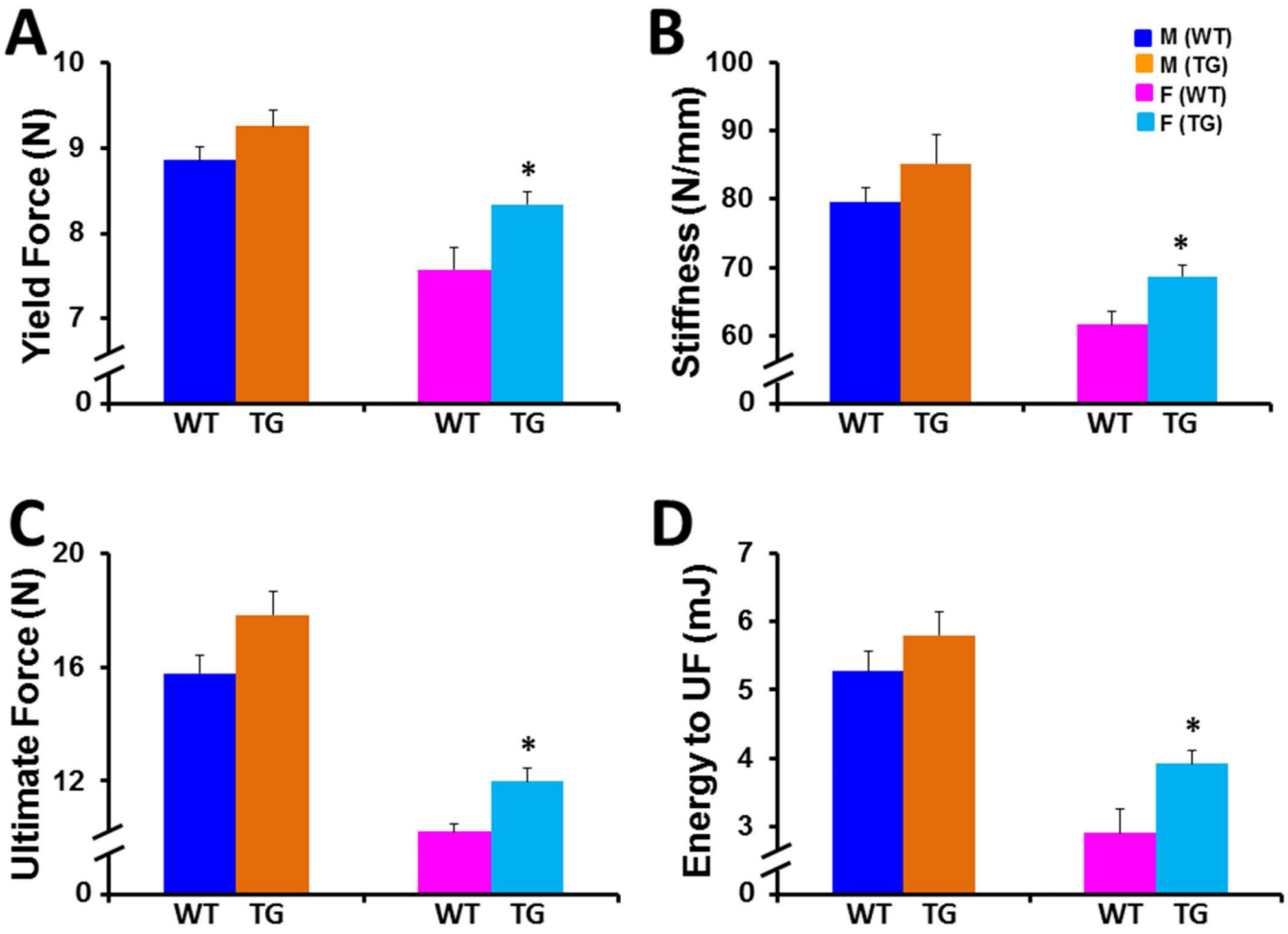

Fig. 6.

Measurement of bone strength by femur biomechanical test. Three-point bending test of femora from 12-wk-old mice demonstrated that female Dmp1-hWNT16 transgenic mice showed significantly higher yield force (6A), stiffness (6B), ultimate force (6C) and energy to ultimate force (6D) as compared to female WT mice. In contrast, male Dmp1-hWNT16 TG mice exhibited similar values for stiffness, ultimate force and energy to ultimate force compared to sex-matched WT mice. Values are given as mean ± SEM vs. *$p<0.05$ corresponding WT using Student's t test. WT: wild-type; TG: Dmp1-hWNT16 transgenic

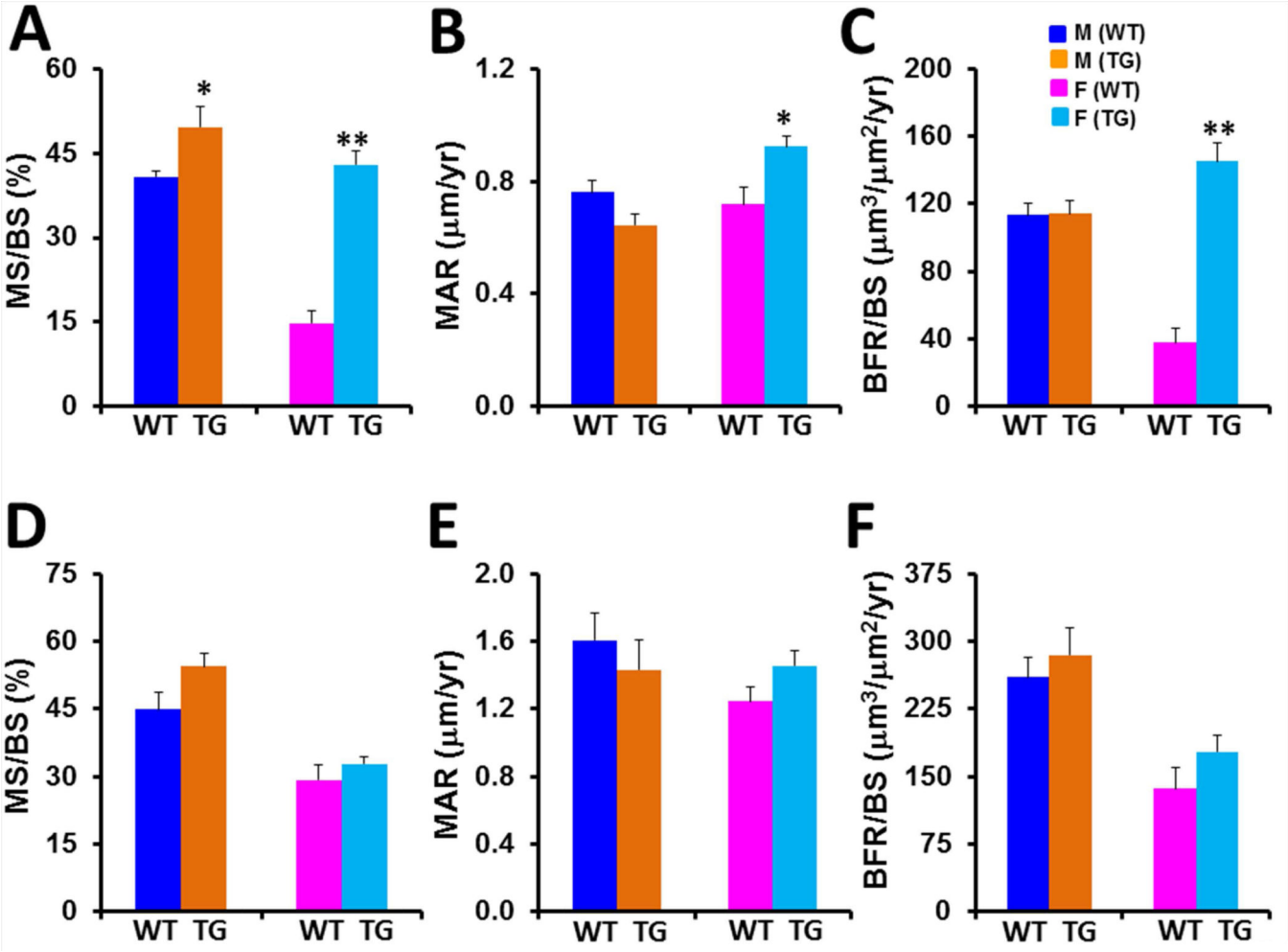

Fig. 7.

Dynamic trabecular and cortical bone histormorphometric measurements. Fluorochrome labeling of trabecular bone from 12-wk-old mice revealed that both male and female Dmp1-hWNT16 transgenic mice had significantly higher distal femur MS/BS compared to WT mice (7A). Female Dmp1-hWNT16 transgenic mice also showed significantly higher MAR (7B) and BFR/BS (7C) compared to sex-matched WT littermates. In femur midshaft, male and female Dmp1-hWNT16 transgenic mice displayed similar values for periosteal MS/BS, MAR and BFR/BS compared to sex-matched WT littermates (7D–F). Values are given as mean ± SEM *$p<0.005$; **$p<0.0005$ vs. corresponding WT using Student's t test. WT: wild-type; TG: Dmp1-hWNT16 transgenic

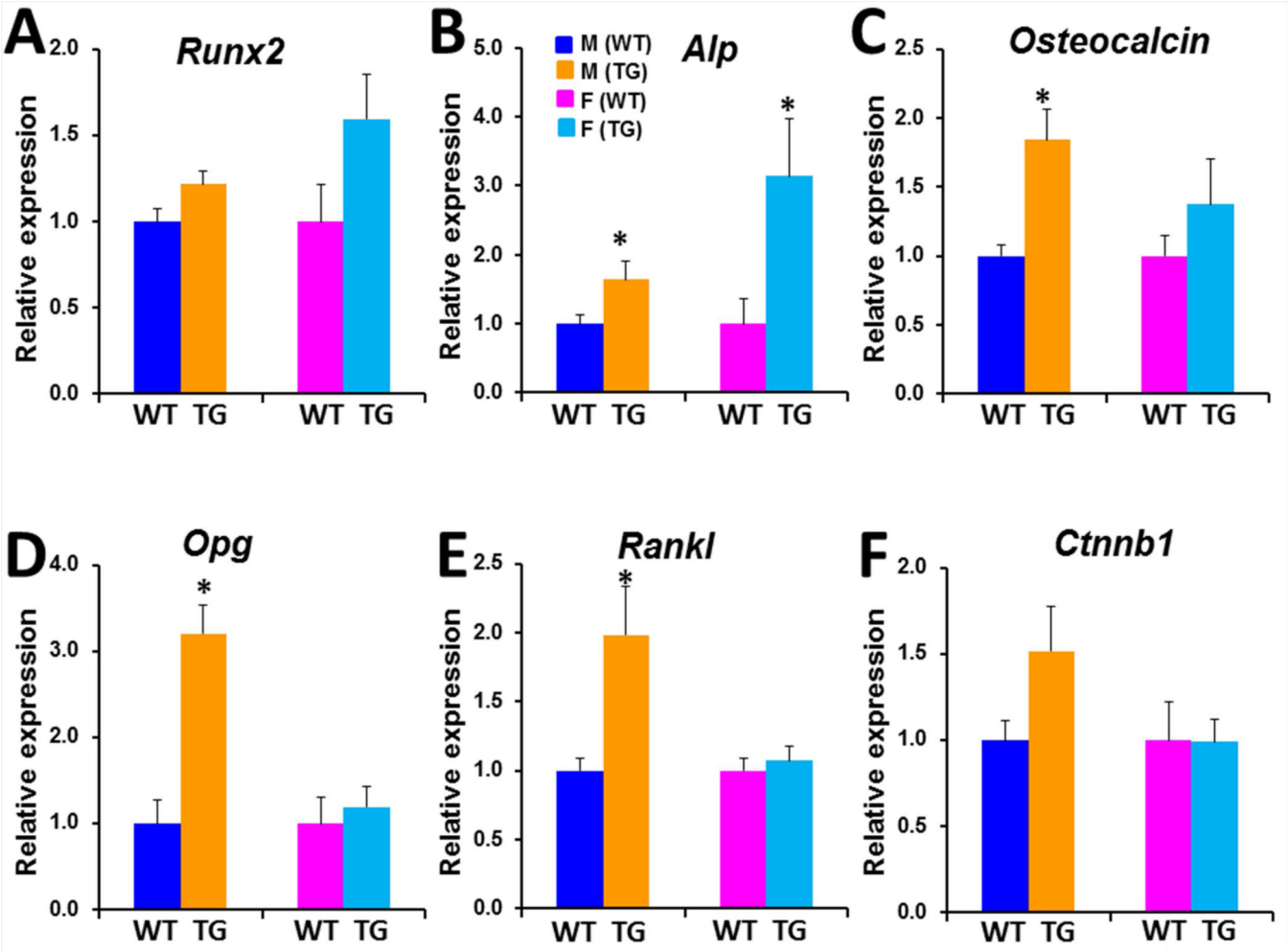

Fig. 8.

Analyses of gene expression in the bone tissue. The mRNA levels of *Alp* was significantly higher in the bone tissue of both male and female Dmp1-hWNT16 transgenic mice compared to the sex-matched WT littermates (8B). The level of *Osteocalcin* expression was significantly higher in male Dmp1-hWNT16 transgenic mice (8C). In addition, expression of *Opg* and *Rankl* were significantly up-regulated in the same tissue in male Dmp1-hWNT16 transgenic mice (8D and 8E) compared to the WT littermates. N=5–6 per sex per genotype. Values are given as mean ± SEM vs. *p<0.05 corresponding WT using Student's t test. WT: wild-type; TG: Dmp1-hWNT16 transgenic

Table 1

Comparison of body weight, bone length, bone density and mineral content in male and female wild-type and transgenic Dmp1-hWNT16 mice [a]

	Male (WT)	Male (TG)	*p-value*	Female (WT)	Female (TG)	*p-value*
Body weight (g)						
6 weeks	20.6 ± 0.62	19.3 ± 0.52	0.39	16.3 ± 0.34	15.8 ± 0.23	0.12
12 weeks	26.0 ± 0.57	25.5 ± 0.47	0.68	19.9 ± 0.39	19.4 ± 0.25	0.21
Femur length (mm)						
6 weeks	14.6 ± 0.08	14.5 ± 0.05	0.59	14.1 ± 0.05	14.0 ± 0.04	0.22
12 weeks	15.4 ± 0.10	15.3 ± 0.10	0.60	14.7 ± 0.10	14.4 ± 0.10	0.14
Whole body BMC (g)						
6 weeks	0.280 ± 0.009	0.313 ± 0.009	*0.03*	0.221 ± 0.009	0.378 ± 0.006	*0.002*
12 weeks	0.468 ± 0.011	0.519 ± 0.014	*0.01*	0.378 ± 0.006	0.457 ± 0.006	*<0.0001*
Femur aBMD (g/cm^2)						
6 weeks	0.0533 ± 0.002	0.0609 ± 0.002	*0.01*	0.0444 ± 0.001	0.0550 ± 0.001	*0.00002*
12 weeks	0.0568 ± 0.001	0.0638 ± 0.001	*0.001*	0.0492 ± 0.001	0.0578 ± 0.001	*<0.0001*
Femur BMC (g)						
6 weeks	0.0187 ± 0.001	0.0203 ± 0.001	*0.26*	0.0133 ± 0.001	0.0173 ± 0.001	*0.0002*
12 weeks	0.0277 ± 0.001	0.0307 ± 0.001	*0.02*	0.0216 ± 0.001	0.0249 ± 0.001	*0.007*
Spine (L1–5) BMC (g)						
6 weeks	0.0237 ± 0.001	0.0269 ± 0.001	*0.01*	0.0207 ± 0.001	0.0252 ± 0.001	*0.004*
12 weeks	0.0378 ± 0.001	0.0436 ± 0.001	*0.02*	0.0344 ± 0.001	0.0434 ± 0.001	*<0.0001*

[a] Values are mean ± SEM; Bold represents significant difference

WT: wild-type; TG: Dmp1-hWNT16 transgenic

Calcif Tissue Int. Author manuscript; available in PMC 2018 April 01.

Table 2

Serum biochemistry and markers of bone formation and resorption in male and female wild-type and transgenic Dmp1-hWNT16 mice [a]

	Male (WT)	Male (TG)	*p-value*	Female (WT)	Female (TG)	*p-value*
Ca (mg/dl)	9.7 ± 0.1	9.8 ± 0.1	*0.55*	9.7 ± 0.1	9.6 ± 0.1	*0.41*
P (mg/dl)	12.2 ± 0.4	12.7 ± 0.5	*0.53*	11.1 ± 0.2	10.9 ± 0.6	*0.68*
BUN (mg/dl)	17.0 ± 0.8	18.4 ± 0.9	*0.26*	18.6 ± 1.0	18.2 ± 0.4	*0.74*
CREA (mg/dl)	0.48 ± 0.01	0.48 ± 0.01	*0.77*	0.46 ± 0.02	0.47 ± 0.02	*0.52*
ALP (U/L)	325.6 ± 12.1	324.7 ± 19.3	*0.97*	353.8 ± 12.0	336.7 ± 14.7	*0.38*
P1NP (ng/ml)	1049 ± 46.4	993 ± 30.2	*0.35*	966 ± 47.7	1007 ± 61.1	*0.61*
OPG (ng/ml)	3566 ± 143.1	3692 ± 99.3	*0.48*	3280 ± 118.9	3215 ± 168.1	*0.74*
RANKL (ng/ml)	119.4 ± 12.0	106.2 ± 9.4	*0.4*	131.6 ± 13.6	130.9 ± 14.8	*0.97*
CTX (ng/ml)	90.9 ± 5.9	134.7 ± 26.9	*0.16*	76.4 ± 12.4	115.3 ± 23.1	*0.12*
TRAcP5b (U/L)	9.8 ± 0.9	9.4 ± 1.0	*0.77*	12.6 ± 0.9	10.5 ± 0.9	*0.1*
CTX/TRAcP5b	11.8 ± 2.3	18.0 ± 4.2	*0.21*	7.0 ± 1.6	13.4 ± 3.6	*0.13*

[a] Values are mean ± SEM

WT: wild-type; TG: Dmp1-hWNT16 transgenic; Ca: calc ium; P: p hosphorus; BUN: blo od urea nitrogen; CRE A: creatinine; ALP: alkaline phosphatase; P1NP: procollagen 1 intact N-terminal; OPG: osteoprotegerin; RANKL: tumor necrosis factor (ligand) superfamily, member 11; CTX: carboxy-terminal collagen crosslinks; TRAcP5b: tartrate-resistant acid phosphatase 5, isoform b